Research on Fast Access Technology Based on Shared Energy Storage of Electric Vehicles

Jin-liang Li[1(✉)], Miao Yang[1], Dai Wan[1], Miao Zhao[1], Jie Tao[2], Shuo Jin[3], and Huisong Ren[4]

[1] State Grid Joint Laboratory for Intelligent Application and Key Equipment in Distribution Network (Hunan), State Grid Hunan Electric Power Company Limted Research Institute, Changsha 410007, Hunan, China
gold921@qq.com
[2] State Grid Changde Power Supply Company, Changde 415000, Hunan, China
[3] Hubei University of Technology, Wuhan 430000, Hubei, China
[4] Hunan Industry Polytechnic, Changsha 410006, Hunan, China

Abstract. Under the background of comprehensively promoting the "dual carbon" strategy, the potential of multiple applications of massive electric vehicles will be fully tapped to carry out electricity protection work with electric vehicles as energy storage medium. At present, users would have short power outage when having access to electric vehicles to restore power supply. In view of this, the fast access technology of electric vehicles and the automatic switching method are presented in this paper, and the corresponding device has been developed. The temperature field simulation analysis and verification of the model were carried out, and the temperature rise test of the device was carried out simultaneously. The method and device has the certain reference value for further research on quick power recovery technology.

Keywords: Electric Vehicles · Fast Access · Emergency Power Supply · Shared Energy Storage · Temperature Field

1 Introduction

At the same time, all kinds of emergency repair tasks are more and more heavy, and a variety of complex electricity consumption scenarios pose great challenges to the emergency power protection work. Especially in towns and other densely populated areas, the traditional single mode of emergency power supply with emergency generator vehicles and diesel generator power protection equipment can no longer meet the reliability, economy and safety requirements of emergency power supply in critical scenarios. This problem can be effectively solved by using electric vehicles instead of traditional electric generators. However, when using electric vehicles to restore power supply, users would have short power outage. The integrated distribution box of the pole-type transformer does not have the function of quick power connection. When the user needs to ensure

H. Yang et al. (Eds.): SmartGIFT 2022, LNICST 483, pp. 432–438, 2023.
https://doi.org/10.1007/978-3-031-31733-0_37

power supply in line maintenance and power failure, a series of preparation work such as power failure, electricity test and grounding need to be completed, and then the bolt fixing method is used to connect the integrated distribution box[1–4]. In view of this problem, this paper puts forward an fast access method of electric vehicles, and the corresponding device is developed that is established on the temperature field simulation analysis and temperature rise test verification.

2 Device Model

The fast access technology of electric vehicles for "quick power recovery" is designed, which includes quick coupling of electric vehicles power, quick switch of ATS dual power supply. It can realize the switch between the main and electric vehicles power at millisecond level (non-inductive). The working principle and structure of the device are shown in Fig. 1.

The design idea of the whole device is as follows:

1) the 380 V main power supply and stand-by power are connected to the outgoing lines through the automatic transfer switch and current transformer. If the main power supply fails, the electric vehicles power will be quickly switched to the low-voltage power supply side through the automatic transfer switch. And the user has no perception in the whole conversion process.
2) The input side of the electric vehicles power of the device adopts the quick coupling. The connection time only needs 2 –3 min to realize the fast access of electric vehicles power, which can greatly improve the efficiency of quick power recovery.
3) In order to ensure better waterproof performance, the quick coupling is set at the bottom of the device.
4) To ensure the safety of mains and electric vehicles power inlet side, fuse type isolating switches are set at both mains and electric vehicles power inlet positions.
5) In order to prevent the risk of insulation damage and interphase short circuit of the bus bar on the same horizontal line, the bus bar of the inlet side is set with cross arrangement.

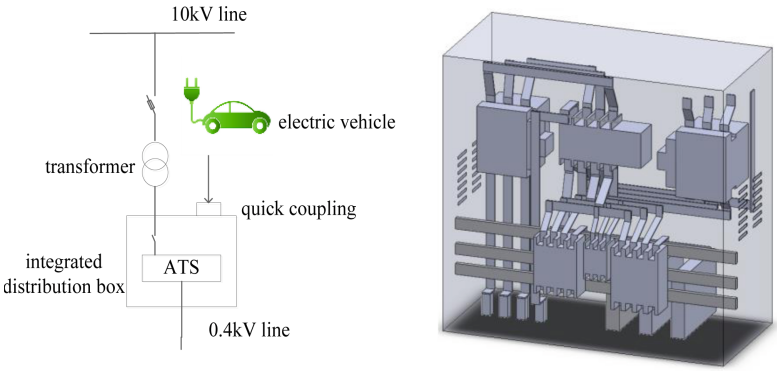

Fig. 1. Schematic diagram of working principle and overall structure drawing of the device

3 Device Model

The temperature rise test is an important test of the integrated distribution box (the corresponding device). The following is a simulation analysis of temperature rise test based on the temperature field.

3.1 Temperature Field Governing Equation

Based on the principle of heat transfer, there are three main forms of heat transfer mechanism between objects: heat conduction, heat convection and heat radiation, and their mathematical description is as follows [5–7]:

1) heat conduction

$$q = -kS\frac{\partial T}{\partial x} \tag{1}$$

In the formula (1), Q is the heat flow per unit area, K is the thermal conductivity, S is the area in the vertical direction of the heat flow density, ∂T/∂X is the temperature gradient in the heat flow direction, and the negative sign indicates that the heat flow direction is always opposite to the positive direction of the temperature gradient.

For a heat transfer system whose temperature does not change with time, that is, a steady-state system, Eq. (1) can be used to describe it. For a heat transfer system whose temperature changes with time, a complete heat conduction equation must be used to describe it. The mathematical expression of the three-dimensional heat conduction equation in the Cartesian coordinate system is as follows:

$$\frac{\partial}{\partial x}\left(k\frac{\partial T}{\partial x}\right)+\frac{\partial}{\partial y}\left(k\frac{\partial T}{\partial \mathrm{y}}\right)+\frac{\partial}{\partial z}\left(k\frac{\partial T}{\partial z}\right)+q' = \rho \mathrm{c}\frac{\partial \mathrm{T}}{\partial \mathrm{t}} \tag{2}$$

In the formula (2), q' is heating rate per unit volume, ρ and C are density and specific heat capacity of the material, respectively.

2) heat convection

$$q = hS(\mathrm{T} - \mathrm{Tf}) \tag{3}$$

In the formula (3), h is the convective heat transfer coefficient, S is the surface area of the wall, T and T_f are the temperature of the wall and the external fluid, respectively. Equation (3) is mainly used to describe the heat transfer between solid wall surface and fluid.

3) heat radiation

$$q = \sigma \varepsilon SF12(\mathrm{T}_1^4 - \mathrm{T}_2^4) \tag{4}$$

In the formula (4), σ is the Stefan-Boltzmann constant with a value of 5.670×10^{-8} W m^{-2} K^{-4}, ε is the emissivity, S is the surface area of the thermal irradiated object, F_{12} is the shape coefficient from the radiant surface to the irradiated surface, T_1 and T_2 are the temperature of the thermal irradiated object and the irradiated object respectively.

3.2 Boundary Conditions

For transient thermal analysis, the setting of boundary conditions and initial conditions is an inevitable requirement for the solution of thermal field and the uniqueness of solution results. The mathematical description of three types of boundary conditions and initial conditions is as follows [8, 9]:

1) the first kind boundary condition

$$T|_{\Gamma} = T(x, y, z, t) \tag{5}$$

In the formula (5), Γ is the boundary of the object. T(x, y, z, t) is the known temperature at any point in the boundary of the object, which can be a constant or a temperature function that varies with the space and time.

2) the second kind boundary condition

$$-k\frac{\partial T}{\partial n}\bigg|_{\Gamma} = q(x, y, z, t) \tag{6}$$

In the formula (6), k is the thermal conductivity coefficient, q (x, y, z, t) is the known heat flux function, also can be a constant. Equation (6) means that the heat flux at the boundary of the object is known.

3) the third kind boundary condition

$$-k\frac{\partial T}{\partial n}\bigg|_{\Gamma} = h(T - T_f)\big|_{\Gamma} \tag{7}$$

In the formula (7), h and T_f are the convective heat transfer coefficient and temperature of the fluid in contact with the object boundary respectively, which can be a constant or a function that varies with space. Equation (7) means that the heat transfer between the boundary of the body and the fluid is known.

4) the initial condition

$$T|_{t=0} = T0(x, y, z) \tag{8}$$

In the formula (8), T_0(x,y,z,t) is the temperature distribution of the object at the initial moment. If it is a constant, it means the temperature distribution of the object is uniform; if it is a known temperature distribution function, it means the temperature distribution is not uniform.

Consider that when the device is running, the current is only distributed inside the current-carrying conductor. The current carrying conductor is the main heat source of device heating. The conductor material is copper, and the resistivity is set to 1.67×10^{-8} Ω m. In addition, to simulate the contact resistance of the device joint, a contact resistance layer of 0.5 mm is set at joints. The resistivity of the contact resistance layer is set to 1×10^{-6} Ω m. The ambient temperature is set to 20 °C. The current of the inlet line side is set to 630 A. The current of the one outlet line side is set to 630 A, and the current of the other outlet line side is set to 0 A.

The convective heat transfer coefficient h of each face of the cabinet is calculated as follows:

$$h = \frac{kN_u}{L} \tag{9}$$

$$Nu = aR_a^b \tag{10}$$

The practical calculation formula of the constant a and b is shown in Table 1.

Table 1. The practical calculation formula of the convection heat transfer in a natural convection system

Surface shape, relative position and direction of heat flow	a	b	Range of application
Vertical cylinder and panel	0.59	1/4	$Ra = 10^4$ --10^9
	0.10	1/3	$Ra = 10^9$-10^{18}
Horizontal cylinder	0.53	1/4	$Ra = 10^4$-10^9
	0.13	1/3	$Ra = 10^9$-10^{12}
Horizontal panel of hot face up	0.54	1/4	$Ra = 10^5$-2×10^7
	0.14	1/3	$Ra = 2 \times 10^7$-3×10^{10}
Horizontal panel of hot face down	0.27	1/4	$Ra = 3 \times 10^5$-3×10^{10}

After calculation, the convective heat transfer coefficient of the top panel is 4.78 W/(m^2 °C), the convective heat transfer coefficient of the side panel is 3.41 W/(m^2 °C), the convective heat transfer coefficient of the bottom panel is 1.74 W/(m^2 °C).

3.3 Simulation Results

According to the above settings, the surface temperature of the equipment inside the device is shown as Fig. 2. The maximum temperature inside the device reaches 89.44 °C, and the maximum temperature rise reaches 69.44 °C. The maximum temperature rise occurs at the B phase inlet line side of the fuse type disconnecting switch.

4 Field Test and Validation

The temperature rise test was carried out on the developed device, and the layout of temperature measuring points of the field temperature rise test is shown in Fig. 3. The measured results of temperature rise test are shown in Table 2. The maximum temperature rise reaches 79.9 °C, and the maximum temperature rise occurs at the B phase inlet line side of the fuse type disconnecting switch similarly. After carrying out the temperature rise test, the electric vehicle access method is simulated and verified.

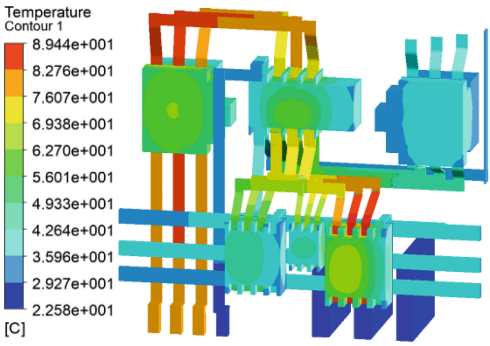

Fig. 2. Simulation results of device surface temperature

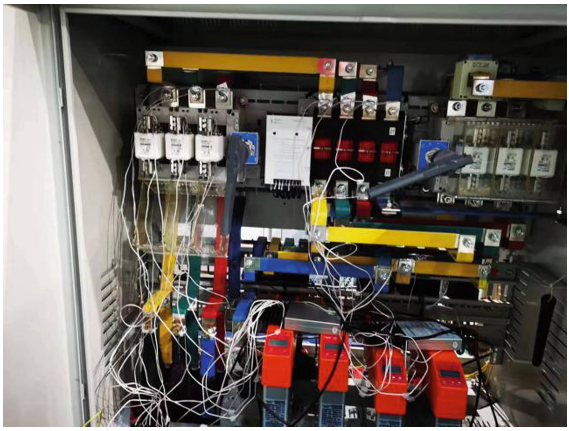

Fig. 3. Layouts **of** temperature measuring points of the field temperature rise test

Table 2. Temperature rise test results

Position	Temperature rise test results (K)		
	A phase	B phase	C phase
The inlet line side of the fuse type disconnecting switch	74.0	79.9	75.6
The outlet line side of the fuse type disconnecting switch	68.3	69.4	67.4
The inlet line side of 630 A circuit breaker	66.9	67.0	64.1
The outlet line side of 630 A circuit breaker	54.0	49.8	52.3
The joint fastening the busbar	39.0	42.5	41.4
The operating handle of the fuse type disconnecting switch	18.7		
The body shell	7.2		

5 Conclusion

It is known that the results of simulation analysis and test are in agreement through the above simulation analysis and experimental verification, and the maximum temperature rise occurs at the B phase inlet line side of the fuse type disconnecting switch similarly. The temperature field simulation can effectively simulate the temperature rise test of the device, and it can be used as an effective method for optimum design of device structure, which can save the production cost and cycle of the device.

The fast access method put forward in this paper and the corresponding developed device can be effectively applied in fast access of electric vehicles, which can be widely used in emergency power protection and transformer live maintenance and replacement scenarios, and users do not have short power outages.

Acknowledgment. This work was financially supported by the science and technology project of State Grid Hunan Electric Power Company Limited (5216A5220003).

References

1. Yang, M., Long, C., Zhou, H.: Development ideas of live working specialty in Hunan Distribution Network. Hunan Electr. Power **40**(03), 42–47 (2020)
2. Fang, J.: Analysis on risk factors and preventive measures of live working management in distribution network. Enterp. Reform Manag. (04), 43–44 (2019)
3. Jiang, Y., Fan, S., Chen, J.: New intelligent technology for live working and its application. Hunan Electr. Power **38**(05), 1–4 (2018)
4. Seaman, A., Dao, T.S., Mcphee, J.: A survey of mathematics-based equivalent-circuit and electrochemical battery models for hybrid and electric vehicle simulation. J. Power Sources **256**(3), 410–423 (2014)
5. Shi, P., Xia, X., Chen, C.: Temperature field of permanent magnet synchronous motor based on coupled field-circuit. J. Nanjing Univ. Aeronaut. Astronaut. **53**(03), 425–434 (2021)
6. Zhou, X., Sun, L., Wang, J.: Temperature rise calculation of permanent magnet synchronous motor based on equivalent heat network method. Micromotors **52**(11), 21–26 (2019)
7. Xu, Y., Ai, M., Yang, Y.: Heat transfer characteristic research based on thermal network method in submersible motor. Int. Trans. Electr. Energy Syst. **28**(3), e2507 (2018)
8. Wang, D., Liang, Y., Li, C., et al.: Thermal equivalent network method for calculating stator temperature of a shielding induction motor. Int. J. Thermal Sci. **147**, 106149 (2020)
9. Li, T., Sun, X.-W., Du, X.-P.: Simulation analysis of transformer flow field and temperature field based on finite element method. Autom. Instrum. **35**(05), 1–6 (2020)